Smart Materials and Structures

PURPOSE-LED PUBLISHING™

PAPER

Theoretical and experimental investigation of the shape memory properties of an ionic polymer–metal composite

To cite this article: Qi Shen *et al* 2017 *Smart Mater. Struct.* **26** 045020

View the article online for updates and enhancements.

You may also like

- Analysis and experiment on a self-sensing ionic polymer–metal composite actuator
Doan Ngoc Chi Nam and Kyoung Kwan Ahn
- Experimental study on strain distribution of ionic polymer–metal composite actuator using digital image correlation
Hongguang Liu, Ke Xiong, Man Wang et al.
- Influence of environmental conditions and voltage application on the electromechanical performance of Nafion-Pt IPMC actuators
Allison M Arnold, Ji Su and Edward M Sabolsky

This content was downloaded from IP address 131.216.14.8 on 07/04/2026 at 18:05

IOP Publishing Smart Materials and Structures
Smart Mater. Struct. 26 (2017) 045020 (8pp) https://doi.org/10.1088/1361-665X/aa61e9

Theoretical and experimental investigation of the shape memory properties of an ionic polymer–metal composite

Qi Shen[1], Viljar Palmre[1], Kwang J Kim[1] and Il-Kwon Oh[2]

[1] Active Materials and Smart Living (AMSL) Laboratory, Mechanical Engineering Department, University of Nevada—Las Vegas, Las Vegas, NV 89154-4027, United States of America
[2] Creative Research Initiative Center for Functionally Antagonistic Nano-Engineering, Department of Mechanical Engineering, Korea Advanced Institute of Science and Technology (KAIST), 291 Daehak-ro, Yuseong-gu, Daejeon 34141, Republic of Korea

E-mail: Kwang.kim@unlv.edu

Received 11 November 2016, revised 15 January 2017
Accepted for publication 21 February 2017
Published 9 March 2017

Abstract

An ionic polymer–metal composite (IPMC) is typically based on a Nafion membrane with electrode plating on both sides and has a promising potential for biomimetic robotics, biomedical devices and human affinity applications. In this paper, the shape memory properties of IPMC were theoretically and experimentally studied. We presented the multiple shape memory properties of a Nafion cylinder. A physics based model of the IPMC was proposed. The free energy density theory was utilized to analyze the shape properties of the IPMC. To verify the model, IPMC samples with Nafion as the base membrane were prepared and experiments were conducted. A simulation of the model was performed and the results were compared with the experimental data. It was successfully demonstrated that the theoretical model can well explain the shape memory properties of the IPMC. The results showed that the reheat glass transition temperature of the IPMC is lower than the programming temperature. It was also found that the back-relaxation of the IPMC decreases as the programming temperature increases. The current study may be useful in order to better understand the shape memory effect of IPMC.

Keywords: ionic polymer–metal composite, shape memory, actuator, Nafion

(Some figures may appear in colour only in the online journal)

1. Introduction

An ionic polymer–metal composite (IPMC) is a type of electroactive polymer [1–3]. It is composed of an ionic polymer membrane with two layers of electrodes chemically plated on both sides [4–9]. Its most significant characteristics are the electro-mechanical and mechano-electrical transactions. The free cations will begin to migrate inside the polymer induced by an applied electric field. The ion distributions will cause the IPMC to generate a large bending deformation. Meanwhile, the mobile cations will distribute if the IPMC has a mechanical deformation. As a result, a detectable electrical signal can be produced at both electrodes. With the capabilities of resilience, inherent softness and biocompatibility, the IPMC has the potential for use as an underwater actuator/sensor. Applications on biomimetic robotics, biomedical devices and energy harvesters have been demonstrated [10–18]. Shape memory polymers are materials that can memorize a permanent shape and then later return to their original shape under specific conditions of external thermal, electrical or other stimulations [19–21]. They have the advantages of high elastic deformation, low cost, low density and potential biocompatibility and biodegradability. Their ability to remember multiple shapes has attracted significant attention from scientists and engineers for the application of actuators, sensors and smart devices [22].

The shape memory properties of IPMC have recently been studied. Xie reported that annealed dry Nafion can be programmed to memorize four different shapes [23]. The permanent shapes were deformed at different temperatures

 © 2017 IOP Publishing Ltd Printed in the UK

and fixed at lower temperatures. By subsequently reheating the Nafion, the programed shapes were obtained respectively. With the broad glass transition range, the Nafion can be potentially programmed in plenty of unique shapes which can be recovered at different temperatures respectively. Rossiter *et al* presented the shape memory properties of Nafion-based IPMC [24]. The IPMC was programmed at the deformation induced by either external force or by electrical actuation. Slow decay was also observed along with the shape memory effect. However, to date, while experimental investigations on the shape memory properties of Nafion-based IPMC have been conducted, few works have been conducted with regards to the theoretical investigation of the shape memory effect of the IPMC. As a result, a poor understanding exists regarding the physics of the shape memory properties of IPMC. A faithful model is desirable to explain the thermo-mechanical transaction phenomenon of IPMC.

In this paper, a demonstration of the shape memory effect of Nafion fiber was firstly developed. Multi-shape programming of the Nafion fiber was conducted and the Nafion fiber was shown to be able to achieve a series of complex shapes. Secondly, a physics-based model of the IPMC was presented. The finite element approach was used to model the mechanical portion of the IPMC. The free energy density theory was used to analyze the shape memory properties of the IPMC. Finally, IPMC strip samples were prepared. Experiments were conducted to test the IPMC strip. Simulation of the model was performed and the results were compared with the experimental data.

2. Results

2.1. Multiple shape memory properties of cylindrical Nafion

Xie has reported the quadruple shape memory properties of a Nafion strip [23]. Compared with the strip, the Nafion cylinder with two dimensions can achieve more complex locomotion. In the current paper, we presented the multiple shape memory properties of a Nafion cylinder. Nafion pellets were heated to above fusion temperature. By extruding the molten Nafion through a brass extruder dye, the cylinder shape of the Nafion was obtained. A Nafion cylinder with a length of 99.87 mm and a diameter of 0.95 mm was fabricated and used for the test. The Nafion cylinder was wrapped around a metal rod and fixed. Triple shapes were programmed with different loops of the Nafion wrapping around the rod in an oven. The cylinder with original shape S0 was wrapped and programmed at 130 °C and fixed at 100 °C to achieve the first programmed shape S1. The second shape S2 was programmed at 100 °C and fixed at 70 °C. By programming the third shape S3 at 100 °C and fixing it at 20 °C, the triple shape programming of the Nafion cylinder was completed.

Then the Nafion cylinder was reheated. The Nafion cylinder recovered to S2′, S1′ and S0′ upon reheating to 70 °C, 100 °C and 130 °C respectively. Figure 1 shows the Nafion cylinder demonstrating quadruple shape memory

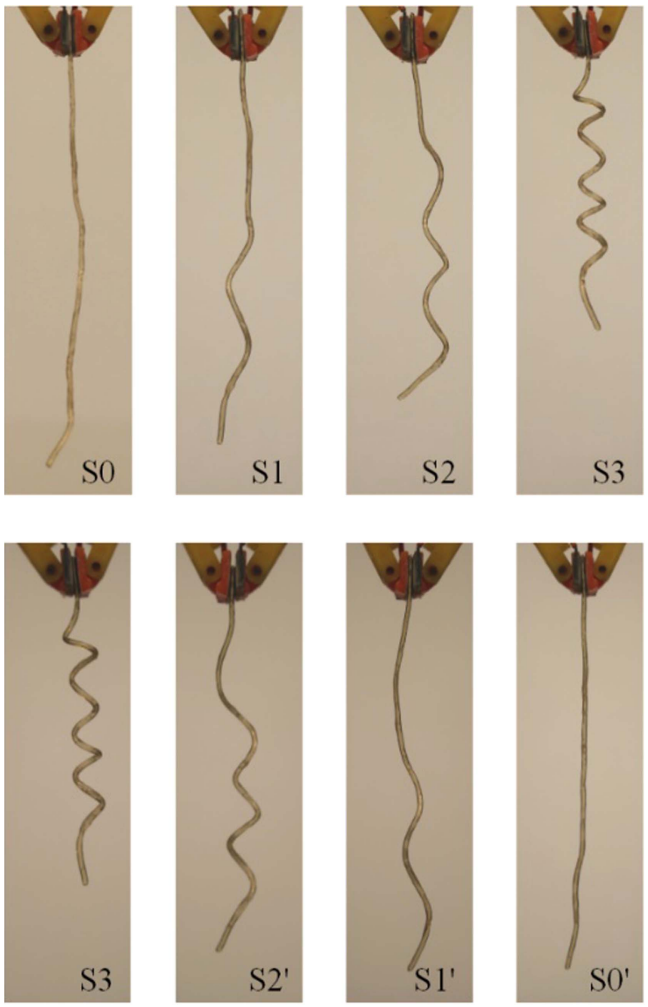

Figure 1. Multiple shape memory properties of the Nafion cylinder.

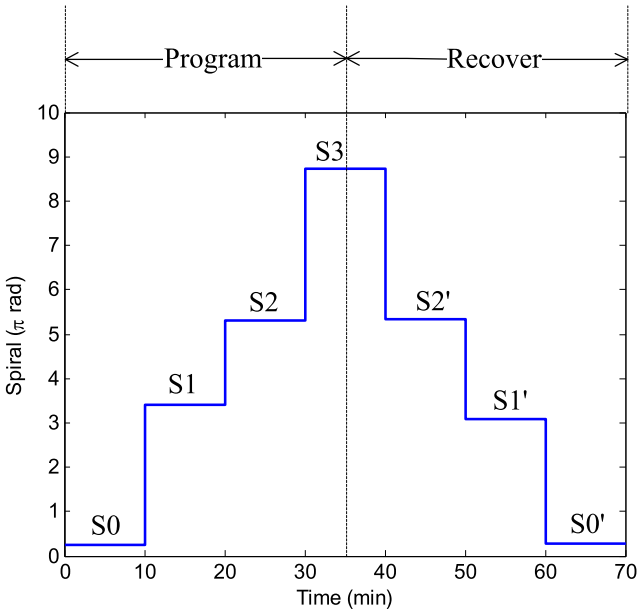

Figure 2. Shape memory cycle of the Nafion cylinder.

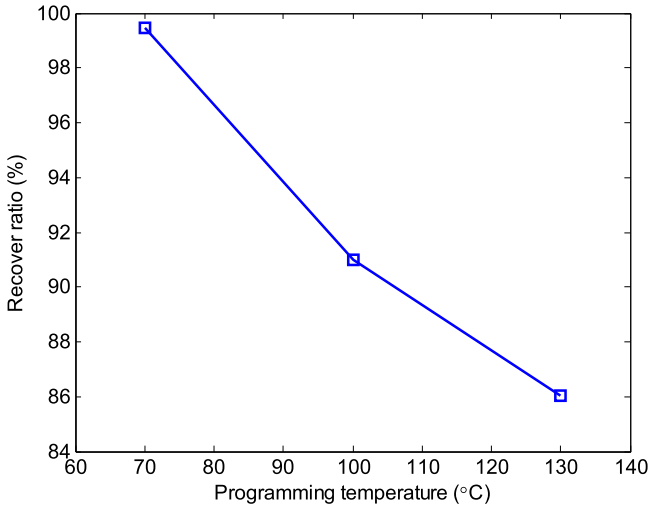

Figure 3. Recovering ratio of the Nafion cylinder at different programming temperatures.

cycles. Figure 2 shows the shape memory cycle of the Nafion cylinder in accordance with figure 1. The spiral of the cylindrical Nafion was programmed to increase during the programming period and decrease as the reheating temperature increased during the recovering period. Figure 3 shows the recovering ratio of the Nafion cylinder at different programming temperatures. It can be seen that as the programming temperature increases, the recovering ratio decreases. Rossiter presented the spiral deformation of the IPMC strip in the shape memory cycle [24]. The Nafion-based IPMC demonstrates a thermo-mechanical shape memory effect but the recovery is not complete. The reasons may be as follows: (1) the IPMC in [24] is based on a thin Nafion membrane. Compared with the cylinder shape of the current paper, the strip is relatively difficult to recover in a spiral deformation. (2) The cylinder in the current study was programmed at a temperature of 130 °C, 100 °C, and 70 °C respectively in a dehydrated status, which is higher than the programming temperature of 60 °C in the hydrated status for the IPMC in [24]. (3) Electrodes were plated on the surface of the IPMC in [24], which will have some plastic effects on the deformation of the strip.

2.2. Modeling of the IPMC

The model of the IPMC is presented. The dynamics of the IPMC strip are described based on the finite element method. The IPMC strip is assumed to satisfy the following restrictions: (1) the IPMC is divided by a series of elements along the direction of thickness, as shown in figure 4. Each element was analyzed and modeled individually. (2) The strain along the length direction λ_l is dominant compared with the strains λ_w, λ_h in the width and thickness directions respectively, and $\lambda_w = \lambda_h$. The strain λ_l of each element is also the main reason causing the bending of the IPMC strip. (3) The length of the midline of the strip is constant. Thus, as the strip bends, the elements on the inner side are compressed and the elements on the outer side are stretched. The size of the original IPMC strip element is L, W, dH. In the current study, we only consider the single shape memory effect. The IPMC was

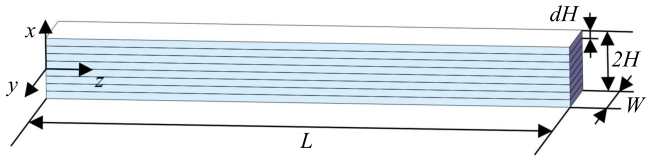

Figure 4. Schematic illustration of the IPMC beam.

programmed at temperature T_1 and cooled in room temperature water. When the IPMC emerged in the water at temperature T, which is above the programming temperature $T > T_1$, the high-temperature water molecule was absorbed into the Nafion, and the IPMC strip recovered its original shape. As a result, the size of the element changes from L, W, dH to l, w, dh. The strain along the z, y, x directions can be expressed as

$$\lambda_l = \frac{l}{L},\ \lambda_w = \frac{w}{W},\ \lambda_h = \frac{\mathrm{d}h}{\mathrm{d}H}. \tag{1}$$

By relating the length of the element to the deformation of the strip, the length can be rewritten as

$$l = (r - t)\frac{\omega(z)}{l} \tag{2}$$

where t is the position of the element in the x direction, $\omega(z)$ is the deformation of the element, r is the radius of the curved IPMC midline and is expressed as

$$r = \frac{l}{\gamma} \tag{3}$$

where γ is the angle of the curved beam and is denoted as

$$\tan\gamma = \frac{\omega(z)}{l}. \tag{4}$$

The nominal stress on the z, y, x directions is denoted as

$$S_l = \frac{F_l}{w\mathrm{d}h} = \sigma_l\lambda_w\lambda_h,\ S_w = \frac{F_w}{l\mathrm{d}h} = \sigma_w\lambda_l\lambda_h,$$
$$S_h = \frac{F_h}{lw} = \sigma_h\lambda_l\lambda_w \tag{5}$$

where σ_l, σ_w, σ_h are the actual stresses and F_l, F_w, F_h are the nominal forces acting on the z, y, x directions. Based on (5), one can obtain [25, 26]

$$\lambda_l\lambda_w\lambda_h = 1 + vC \tag{6}$$

where v is the volume per water molecule, and C is the nominal concentration of the solvent in the polymer matrix. Gibbs first developed the theory of free-energy density to describe the behavior of swelling gel [27]. Flory presented the free-energy function for polymeric gels [28]. The Flory theory was later extended to polyelectrolyte gels [29–31]. The free energy density E of the element can be expressed as [28]

$$E = E_\mathrm{s} + E_\mathrm{m} + E_\mathrm{p} + E_\mathrm{ion} \tag{7}$$

where E_s is the stretching free-energy, E_m is the mix free-energy, E_p is the polarizing free-energy, and E_ion is the ion transporting free-energy. Since no ions in the water move inside the matrix of the polymer, the mix free-energy is $E_\mathrm{ion} = 0$. Assuming that the dielectric constants of the nonpolar polymer and nonpolar water are equivalent, the free

Table 1. Dimensions of the IPMC samples.

Item	L (mm)	W (mm)	$2h$ (mm)
IPMC 1	51.07	9.94	0.57
IPMC 2	37.05	9.94	0.57
IPMC 3	22.16	9.94	0.57

energy polarizing the polymer is $W_p = 0$. Based on Flory's theory, (7) can be rewritten as [28]

$$E = \frac{1}{2}NkT(\lambda_l^2 + \lambda_w^2 + \lambda_h^2 - 3 - 2\log\lambda_l\lambda_w\lambda_h) - \frac{kT}{v}\left[vC\log\left(1 + \frac{1}{vC}\right) + \frac{\chi}{1 + vC}\right] \quad (8)$$

where N is the number of polymer chains divided by the volume of the polymer element, $k = 1.38 \times 10^{-23}$ J K^{-1} is the Boltzmann constant, T is the absolute temperature, and χ is the enthalpy constant during the mixture of the polymer matrix and the solvent. The differentiation of (8) can be written as [26]

$$\frac{\partial E}{\partial\lambda_l} = \frac{kT}{v}\left(Nv\left(\lambda_l\left(1 + \frac{2}{D^2}\right) - \frac{3}{\lambda_l}\right) + \left(\frac{3\lambda_l^2}{D^2}\log\left(1 - \frac{D^2}{\lambda_l^3}\right) + \frac{3}{\lambda_l} + \frac{3\chi D^2}{\lambda_l^4}\right)\right) \quad (9)$$

where D is the ratio between the strain in the z direction and the strain in the x and y directions respectively, and is expressed as

$$D = \frac{\lambda_l}{\lambda_w} = \frac{\lambda_l}{\lambda_h} \geqslant 1. \quad (10)$$

After the deformation of the element in water, the mixture system free energy density of the polymer and the water is expressed as

$$G = E(\lambda_l, \lambda_w, \lambda_h)lw\mathrm{d}h - F_l(l - L) - F_w(w - W) - F_h(\mathrm{d}h - \mathrm{d}H). \quad (11)$$

The free energy combines the enthalpy and entropy. The mixture system tends to be stable as the polymer and the solvent are mixed. When the whole system reaches a steady status, a key assumption is that the system free energy achieves the minimum. The differentiation of the free energy G reaches the minimum. With a small variation, the strain λ_l, λ_w, λ_h can be expanded to $\lambda_l + \delta\lambda_l$, $\lambda_w + \delta\lambda_w$, $\lambda_h + \delta\lambda_h$. The mixture system free energy density is rewritten as [26]

$$\frac{\partial G}{lw\mathrm{d}h} = \left[\frac{\partial E}{\partial\lambda_l} - S_l\right]\delta\lambda_l + \left[\frac{\partial E}{\partial\lambda_w} - S_w\right]\delta\lambda_w + \left[\frac{\partial E}{\partial\lambda_h} - S_h\right]\delta\lambda_h + \frac{\partial^2 E}{\partial\lambda_l^2}\partial\lambda_l^2 + \frac{\partial^2 E}{\partial\lambda_w^2}\partial\lambda_w^2 + \frac{\partial^2 E}{\partial\lambda_h^2}\partial\lambda_h^2 + \frac{\partial^2 E}{\partial\lambda_l\partial\lambda_w}\partial\lambda_l\partial\lambda_w + \frac{\partial^2 E}{\partial\lambda_w\partial\lambda_h}\partial\lambda_w\partial\lambda_h + \frac{\partial^2 E}{\partial\lambda_l\partial\lambda_h}\partial\lambda_l\partial\lambda_h. \quad (12)$$

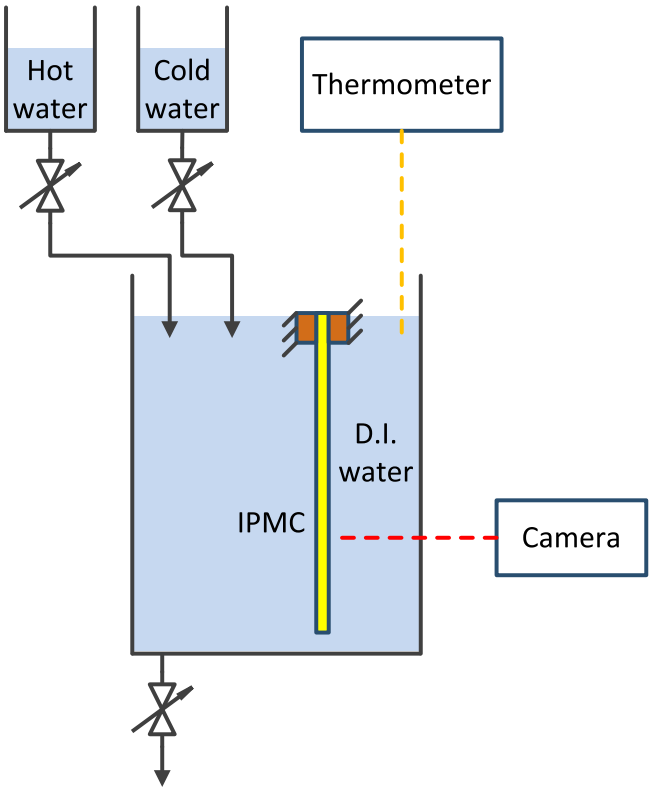

Figure 5. Experimental set up for the shape memory properties.

To achieve the minimum of (12), the first-order differential functions of (12) are assigned zero. One can obtain

$$S_l = \frac{\partial E}{\partial\lambda_l},\ S_w = \frac{\partial E}{\partial\lambda_w},\ S_h = \frac{\partial E}{\partial\lambda_h}. \quad (13)$$

By integrating the length direction stress of the element, the total length direction stress on the IPMC strip can be expressed as

$$\sigma = \int_{-h}^{h}\sigma_l\mathrm{d}t = \int_{-h}^{h}\frac{S_l}{\lambda_w\lambda_h}\mathrm{d}t. \quad (14)$$

By relating the bending moment on the IPMC strip to the induced stress, one can obtain

$$\sigma = \frac{Mh}{I} \quad (15)$$

where I is the moment of inertia of the strip and $I = 2/3wh^3$. Based on the linear beam theory, the relation between the displacement ω of the strip and the bending moment M can be denoted as [32]

$$\frac{\partial^2\omega(z)}{\partial z^2} = \frac{M}{YI} \quad (16)$$

where Y is the Young's Modulus. By combining (14), (15) and (16), an ordinary differential equation (ODE) of $\omega(z)$ is obtained. The boundary conditions of the ODE are $\omega(0) = 0$ and $\partial\omega(0)/\partial z = 0$. By solving the ODE, the deformation $\omega(z)$ of IPMC can be obtained. MATLAB was used to solve $\omega(z)$.

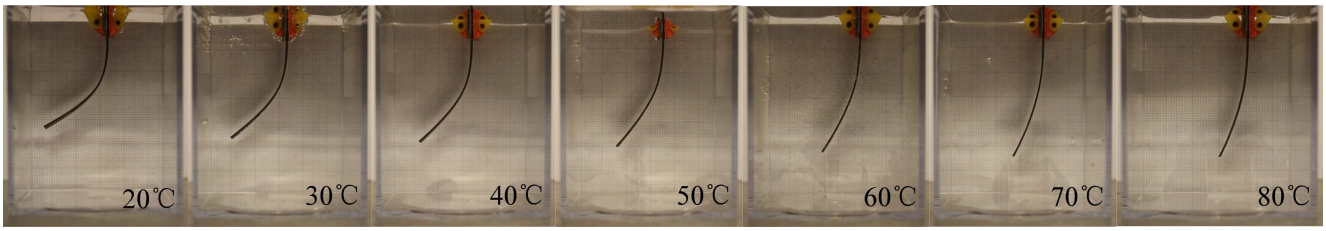

Figure 6. The thermo-mechanical shape of IPMC at different temperatures.

2.3. Experimental verification

Experiments were conducted to study the shape memory effect of the IPMC. Three IPMC samples were utilized for the experiments. The dimensions are shown in table 1. The sample was curved in a fixture and held in place during the programming period. The first step was to immerse the IPMC strip in a hot water bath with the programming temperature T_{p} ranging from 50 °C–70 °C. Then it was cooled in room temperature water at the fixing temperature T_{f} of 20 °C. Finally the fixture was removed and the IPMC sample was fixed at the curved shape. A back-relaxation of the IPMC sample was noticed after the fixture was removed and the back-relaxation deformation was different at different programming temperatures. Figure 5 shows the experimental set up for the shape memory study. The sample was clamped vertically at one end and immersed in a water tank at different temperatures T_t from 20 °C–80 °C. The tank could be filled with hot water and cold water to the desired temperature. A thermometer was used to measure the temperature of the water during the experiments. The tip displacement of the sample was measured with the grid paper attached to the water tank. The IPMC was measured every 10 min after the water was reheated to the next temperature. The experiments were repeated three times.

Figure 6 shows the deformation of the IPMC strip at different temperatures under the programming temperature T_{p} of 60 °C. The thermo-mechanical shape memory effect was presented. It can be seen that as the reheating temperature increased, the programmed IPMC gradually relaxed back to its original shape. Shahinpoor presented the radius of the curvature ρ_r of IPMC beam as [33]

$$\rho_r \cong \frac{l^2 + \omega^2}{2\omega}. \tag{17}$$

The radius of the curvature ρ_r is in turn related to the maximum tensile (positive) or compressive (negative) strains, which can be expressed as

$$\varepsilon \cong \frac{h}{\rho_r}. \tag{18}$$

The shape recovery ratio of the IPMC sample can be expressed as

$$r_s = \frac{\varepsilon_t - \varepsilon_p}{\varepsilon_r - \varepsilon_p} \times 100\% \tag{19}$$

where ε_t is the strain under current temperature, ε_p is the strain at the fixing temperature of 20 °C and ε_r is the strain at the final reheat temperature of 80 °C. Similar definitions were presented in [23, 34].

Figure 7 shows the comparison of the experimental results and simulation results of the shape recovery of different IPMC samples. The temperature varies from 20 °C–80 °C. It is found that the model can well describe the experimental data. Based on figure 7, it can be seen that as the temperature constantly increases, initially the shape recovery increases gradually and then it rises rapidly. Finally, the sample slowly recovers its original shape. The shape recovery decreases as the programming temperature increases, which is in good agreement with figure 3. It was also noted that the reheat temperature of the glass transition is lower than the programming temperature. Compared with the shape recovery ratio of the Nafion cylinder shown in figure 3, it can be seen that the shape recovery ratio of the IPMC strip is generally lower than that of the Nafion cylinder. One explanation is that the plastic deformation of the metal electrodes plated on the surface of the IPMC strip during the programming phase inhibit its recovery.

Figure 8 shows the back-relaxation deformation of the IPMC samples at different programming temperatures. When the fixture was removed from the IPMC sample, back-relaxation occurred and there is a difference between the desired shape with the fixture and the actually programmed shape without the fixture. It was found that as the programming temperature increased, the IPMC samples have a decreasing back-relaxation. Considering the results of figure 6, it is demonstrated that by increasing the programming temperature, the fixed shape of the IPMC is closer to the desired shape, and less close to its original shape when the IPMC recovered.

3. Discussion

3.1. Application of thermo-mechanical transaction

IPMCs have received significant attention as soft biomimetic actuators/sensors [35, 36]. Tremendous work has been conducted on their application in the fields of biomimetic robotics, biomedical devices and human affinity applications, such as underwater robots, active catheters and underwater soft sensors [13, 37]. Although the shape memory properties of the Nafion-based IPMC have been experimentally investigated, little work has been done on its potential applications or demonstrations. In this paper, a demonstration that uses the thermo-mechanical shape memory properties of Nafion fiber was presented. The demonstration has shown the capability of Nafion fiber to achieve a series of complex shapes with multiple shape programming. These results indicate that the

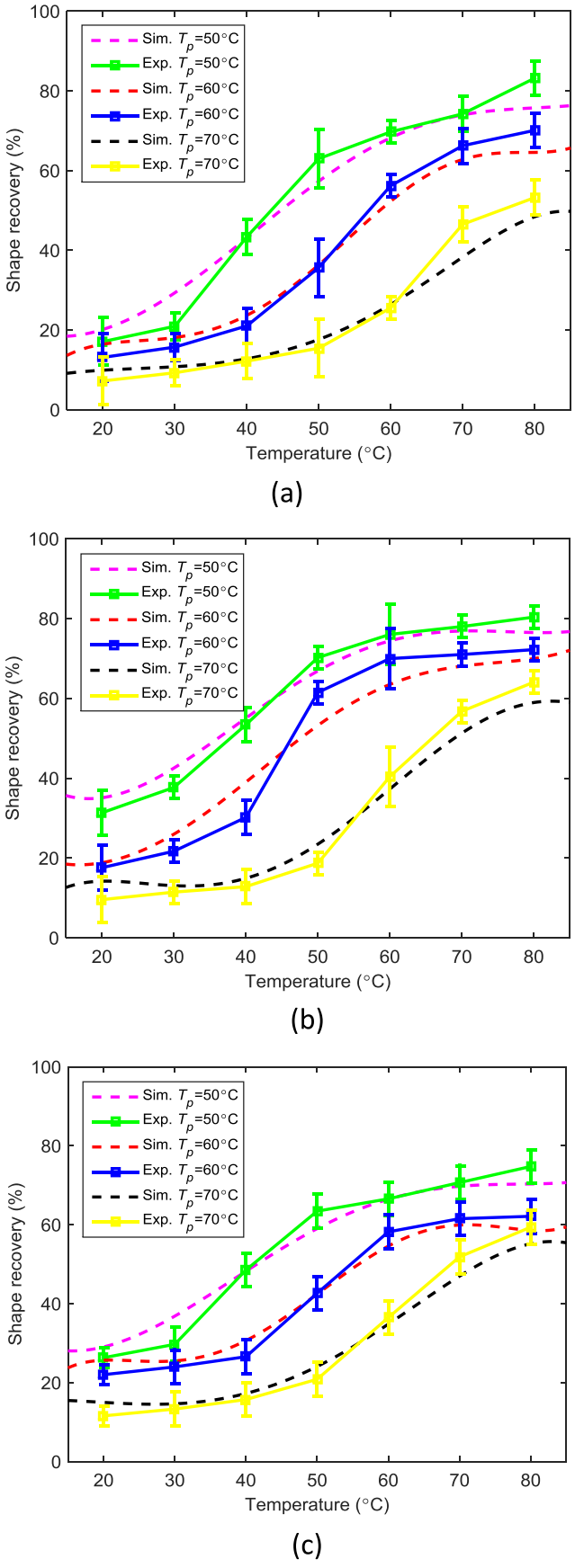

Figure 7. Comparison of the simulation and experimental results of the IPMC shape recovery at different programming temperatures: (a) IPMC 1; (b) IPMC 2; (c) IPMC 3.

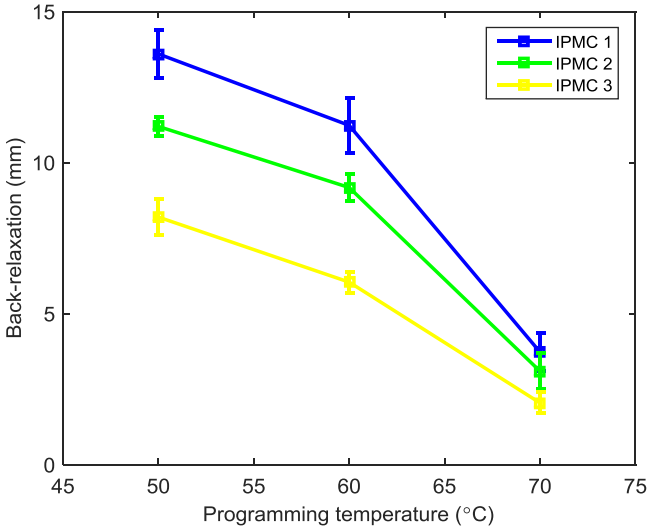

Figure 8. Back-relaxation deformation of the IPMC at different programming temperatures.

thermo-mechanical transaction phenomenon of the Nafion can be potentially applied in the field of biomedical and human affinity devices, including active cannulas, and soft catheters. Previous works have demonstrated the thermo-electrical shape memory properties of the IPMCs [24, 38]. Thermo-electrical shape memory programming was performed. By plating electrodes on the surface of the Nafion, the electro-mechanical/mechano-electrical properties and the thermo-mechanical properties of IPMC can be coupled. More interesting actuating/sensing demonstrations can be presented in the near future. It was also noticed that in both the current paper and previous works, to achieve the shape recovery, the temperature of the IPMC was changed by changing the liquid surrounding it, which is not applicable in the real world. To solve this problem, a thermoelectric cooler will be utilized for the fast programming heating and fixing cooling during the actuation responses of IPMC.

3.2. Model of the shape memory properties

Considerable efforts have been made to describe the electro-mechanical transaction of IPMC [39–42], such as the swelling theory where the migration of the hydrated water results in the deformation of the IPMC [43–46], the influence of the electrode conductivity on the transduction behavior of IPMC [47], the cation redistribution which results in electrostatic stress [48–51], the effect of the electrodes on the charge dynamics of IPMC [52], and the interference between the IPMC surface electrode and the membrane [53, 54]. The mechano-electrical transaction of IPMC has also been studied [55], for instance, underwater object tracking [56, 57], energy harvesting [58, 59], surface electrode sensing [60, 61] and parametric effects [62]. Most of the models are based on the ionic immigration induced by an electric field for actuating, and the concentration variation of ions results from Nafion deformation for sensing. Regarding the thermo-mechanical transactions of IPMC, the ion migration is not the major factor which results in the deformation of the IPMC. To explain this phenomenon, the free energy density

theory was utilized. The volume swelling/shrinking of the Nafion membrane and the temperature variation results in the shape recovery. Through experiments, the results show that the proposed model can well describe the thermo-mechanical transactions of Nafion-based IPMC. The current study is beneficial for identifying the mechanism behind the shape memory feature of IPMC.

4. Methods

4.1. Sample preparation

IPMC strip samples were prepared for the experimental validation. The surface of the Nafion^{TM}-117 membrane sheet was polished and the membrane was immersed in 3% hydrogen peroxide (H_2O_2) to eliminate organic impurities and in 1 M sulfuric acid (H_2SO_4) to remove the metallic impurities. Then the membrane sheet was plated with platinum metal particles by being immersed in a platinum complex solution ($Pt(NH_3)_4Cl_2 \cdot H_2O$), and after that it was immersed in a sodium borohydride solution ($NaBH_4$). To lower the surface resistance, the sheet was suspended in the solution with hydrazine ($NH_2NH_2 \cdot H_2O$) and hydroxylamine hydrochloride ($H_2NOH \cdot HCl$) added to the solution. After the plating process, the sheet was soaked in a solution of lithium chloride (LiCl) for the ion exchange.

4.2. Parameter identification

To perform the simulation of the theoretical model, the parameters need to be identified. Some parameters can be measured directly, such as the dimensions of the IPMC sample and the temperature. Some are physical constants, such as the Boltzmann constant. The rest need to be identified, such as the enthalpy constant. In the current study, the parameters of the model were identified based on the experimental results using the least-square method in MATLAB. For each programming temperature, the parameters were identified separately.

Acknowledgments

This material is based in part upon work supported by the National Science Foundation under grant number #1545857. Any opinions, findings, and conclusions or recommendations expressed in this material are those of the author(s) and do not necessarily reflect the views of the National Science Foundation. Also, KJK acknowledges the partial financial support from the Office of Naval Research (N00014-16-1-2356) for fabrication of IPMC. IKO: This work was, in part, supported by Creative Research Initiative Program (2015R1A3A2028975) funded by National Research Foundation of Korea (NRF).

References

[1] Palmre V, Pugal D, Kim K J, Leang K K, Asaka K and Aabloo A 2014 Nanothorn electrodes for ionic polymer-metal composite artificial muscles *Sci. Rep.* **4** 6176
[2] Pugal D, Kim K J, Punning A, Kasemägi H, Kruusmaa M and Aabloo A 2008 A self-oscillating ionic polymer-metal composite bending actuator *J. Appl. Phys.* **103** 84908
[3] Bhandari B, Lee G Y and Ahn S H 2012 A review on IPMC material as actuators and sensors: fabrications, characteristics and applications *Int. J. Precis. Eng. Manuf.* **13** 141–63
[4] Jo C, Pugal D, Oh I-K, Kim K J and Asaka K 2013 Recent advances in ionic polymer–metal composite actuators and their modeling and applications *Prog. Polym. Sci.* **38** 1037–66
[5] Shahinpoor M and Kim K J 2001 Ionic polymer—metal composites: I. Fundamentals *Smart Mater. Struct.* **819** 819
[6] Shahinpoor M and Kim K J 2005 Ionic polymer–metal composites: IV. Industrial and medical applications *Smart Mater. Struct.* **14** 197–214
[7] Shahinpoor M, Bar-Cohen Y, Simpson J O and Smith J 1998 Ionic polymer-metal composites (IPMCs) as biomimetic sensors, actuators and artificial muscles—a review *Smart Mater. Struct.* **7** R15–30
[8] Shahinpoor M and Kim K J 2004 Ionic polymer–metal composites: III. Modeling and simulation as biomimetic sensors, actuators, transducers, and artificial muscles *Smart Mater. Struct.* **13** 1362–88
[9] Wang Y, Chen H, Wang Y, Zhu Z and Li D 2014 Effect of dehydration on the mechanical and physicochemical properties of gold- and palladium-ionomeric polymer-metal composite (IPMC) Actuators *Electrochim. Acta* **129** 450–8
[10] Shen Q *et al* 2012 On the thrust efficiency of an IPMC actuated robotic swimmer: dynamic modeling and experimental investigation *The 22nd Int. Offshore and Polar Engineering Conf.*
[11] Shen Q, Wang T, Wen L and Liang J 2013 Modelling and fuzzy control of an efficient swimming ionic polymer-metal composite actuated robot *Int. J. Adv. Robot. Syst.* **10** 1–13
[12] Wang T, Shen Q, Wen L and Liang J 2012 On the thrust performance of an ionic polymer-metal composite actuated robotic fish: modeling and experimental investigation *Sci. China Technol. Sci.* **55** 3359–69
[13] Shen Q, Wang T, Liang J and Wen L 2013 Hydrodynamic performance of a biomimetic robotic swimmer actuated by ionic polymer–metal composite *Smart Mater. Struct.* **22** 75035
[14] Shen Q, Wang T, Wen L, Liang J, Yang X and Yao G 2013 A novel method for investigating the kinematic effect on the hydrodynamics of robotic fish *IEEE Int. Conf. on Robotics and Biomimetics (ROBIO)* pp 1306–11
[15] Fang B K, Ju M S and Lin C C K 2007 A new approach to develop ionic polymer-metal composites (IPMC) actuator: fabrication and control for active catheter systems *Sensors Actuators A* **137** 321–9
[16] Giacomello A and Porfiri M 2011 Underwater energy harvesting from a heavy flag hosting ionic polymer metal composites *J. Appl. Phys.* **109** 84903
[17] Cha Y, Verotti M, Walcott H, Peterson S D and Porfiri M 2013 Energy harvesting from the tail beating of a carangiform swimmer using ionic polymer-metal composites *Bioinspir. Biomim.* **8** 36003
[18] Kim K J, Palmre V, Stalbaum T, Hwang T, Shen Q and Trabia S 2016 Promising developments in marine applications with artificial muscles: electrodeless artificial cilia microfibers *Mar. Technol. Soc. J.* **50** 24–34

[19] Lendlein A, Jiang H, Junger O and Langer R 2005 Light-induced shape-memory polymers *Nature* **434** 879–82
[20] Koerner H, Price G, Pearce N A, Alexander M and Vaia R A 2004 Remotely actuated polymer nanocomposites—stress-recovery of carbon-nanotube-filled thermoplastic elastomers *Nat. Mater.* **3** 115–20
[21] Liu C, Qin H and Mather P T 2007 Review of progress in shape-memory polymers *J. Mater. Chem.* **17** 1543–58
[22] Liu C, Chun S B, Mather P T, Zheng L, Haley E H and Coughlin E B 2002 Chemically cross-linked polycyclooctene: synthesis, characterization, and shape memory behavior *Macromolecules* **35** 9868–74
[23] Xie T 2010 Tunable polymer multi-shape memory effect *Nature* **464** 267–70
[24] Rossiter J, Takashima K and Mukai T 2012 Shape memory properties of ionic polymer—metal composites *Smart Mater. Struct.* **21** 112002
[25] Lv H, Leng J, Liu Y and Du S 2008 Shape-memory polymer in response to solution *Adv. Eng. Mater.* **10** 592–5
[26] Lu H, Liu Y, Leng J and Du S 2009 Qualitative separation of the effect of the solubility parameter on the recovery behavior of shape-memory polymer *Smart Mater. Struct.* **18** 85003
[27] Gibbs J W 1906 *The Scientific Papers of J. Willard Gibbs* vol 1 (London: Longmans Green)
[28] Flory P J 1953 *Principles of Polymer Chemistry* (Ithaca: Cornell University Press)
[29] Ricka J and Tanaka T 1984 Swelling of ionic gels: quantitative performance of the Donnan theory *Macromolecules* **17** 2916–21
[30] Hooper H H, Baker J P, Blanch H W and Prausnitz J M 1990 Swelling equilibria for positively ionized polyacrylamide hydrogels *Macromolecules* **23** 1096–104
[31] Brannon-Peppas L and Peppas N A 1991 Equilibrium swelling behavior of pH-sensitive hydrogels *Chem. Eng. Sci.* **46** 715–22
[32] Shen Q, Palmre V, Stalbaum T and Kim K J 2015 A comprehensive physics-based model encompassing variable surface resistance and underlying physics of ionic polymer-metal composite actuators *J. Appl. Phys.* **118** 124904
[33] Shahinpoor M 2003 Ionic polymer-conductor composites as biomimetic sensors, robotic actuators and artificial muscles —a review *Electrochim. Acta* **48** 2343–53
[34] Li J, Viveros J A, Wrue M H and Anthamatten M 2007 Shape-memory effects in polymer networks containing reversibly associating side-groups *Adv. Mater.* **19** 2851–5
[35] Trabia S, Hwang T and Kim K J 2016 A fabrication method of unique Nafion® shapes by painting for ionic polymer–metal composites *Smart Mater. Struct.* **25** 85006
[36] Zhao D, Li D, Wang Y and Chen H 2016 Improved manufacturing technology for producing porous Nafion for high-performance ionic polymer—metal composite actuators *Smart Mater. Struct.* **25** 75043
[37] Chae W, Cha Y, Peterson S D and Porfiri M 2015 Flow measurement and thrust estimation of a vibrating ionic polymer metal composite *Smart Mater. Struct.* **24** 95018
[38] Shen Q, Trabia S, Stalbaum T, Palmre V, Kim K and Oh I 2016 A multiple-shape memory polymer-metal composite actuator capable of programmable control, creating complex 3D motion of bending, twisting, and oscillation *Sci. Rep.* **6** 24462
[39] He Q, Yu M, Zhang X and Dai Z 2013 Electromechanical performance of an ionic polymer–metal composite actuator with hierarchical surface texture *Smart Mater. Struct.* **22** 55001
[40] Kanno R, Tadokoro S, Takamori T, Hattori M and Oguro K 1996 Linear approximate dynamic model of ICPF (ionic conducting polymer gel film) actuator *Proc. IEEE Int. Conf. on Robotics and Automation* **1** 219–25
[41] Zhu Z, Wang Y, Liu Y, Asaka K, Sun X, Chang L and Lu P 2016 Application-oriented simplification of actuation mechanism and physical model for ionic polymer-metal composites *J. Appl. Phys.* **120** 34901
[42] Chang L, Asaka K, Zhu Z, Wang Y, Chen H and Li D 2014 Effects of surface roughening on the mass transport and mechanical properties of ionic polymer-metal composite *J. Appl. Phys.* **115** 244901
[43] Tadokoro S, Yamagami S, Takamori T and Oguro K 2000 Modeling of Nafion-Pt composite actuators (ICPF) by ionic motion *SPIE's 7th Annual Int. Symp. on Smart Structures and Materials* vol 3987, pp 92–102
[44] Gong Y, Tang C, Tsui C and Fan J 2009 Modelling of ionic polymer—metal composites by a multi-field finite element method *Int. J. Mech. Sci.* **51** 741–51
[45] Toi Y and Kang S-S 2005 Finite element analysis of two-dimensional electrochemical–mechanical response of ionic conducting polymer–metal composite beams *Comput. Struct.* **83** 2573–83
[46] Yamaue T, Mukai H, Asaka K and Doi M 2005 Electrostress diffusion coupling model for polyelectrolyte gels *Macromolecules* **38** 1349–56
[47] Shahinpoor M and Kim K J 2000 The effect of surface-electrode resistance on the performance of ionic polymer-metal composite (IPMC) artificial muscles *Smart Mater. Struct.* **9** 543–51
[48] Nemat-Nasser S and Li J Y 2000 Electromechanical response of ionic polymer-metal composites *J. Appl. Phys.* **87** 3321
[49] Porfiri M 2008 An electromechanical model for sensing and actuation of ionic polymer metal composites *Smart Mater. Struct.* **18** 15016
[50] Feng G 2010 Numerical study on dynamic characteristics of micromachined ionic polymer metal composite devices based on molecular-scale modeling *Comput. Mater. Sci.* **50** 158–66
[51] Chen Z and Tan X 2008 A control-oriented and physics-based model for ionic polymer–metal composite actuators *IEEE/ASME Trans. Mechatronics* **13** 519–29
[52] Porfiri M 2009 Influence of electrode surface roughness and steric effects on the nonlinear electromechanical behavior of ionic polymer metal composites *Phys. Rev. E* **79** 1–13
[53] Kim S J, Kim S-M, Kim K J and Kim Y H 2007 An electrode model for ionic polymer–metal composites *Smart Mater. Struct.* **16** 2286–95
[54] Pugal D, Kim K J and Aabloo A 2011 An explicit physics-based model of ionic polymer-metal composite actuators *J. Appl. Phys.* **110** 84904
[55] Chen Z, Tan X, Will A and Ziel C 2007 A dynamic model for ionic polymer–metal composite sensors *Smart Mater. Struct.* **16** 1477–88
[56] Abdulsadda A T and Tan X 2012 An artificial lateral line system using IPMC sensor arrays *Int. J. Smart Nano Mater.* **3** 226–42
[57] Abdulsadda A T and Tan X 2013 Underwater tracking of a moving dipole source using an artificial lateral line: algorithm and experimental validation with ionic polymer–metal composite flow sensors *Smart Mater. Struct.* **22** 45010
[58] Aureli M, Prince C, Porfiri M and Peterson S D 2009 Energy harvesting from base excitation of ionic polymer metal composites in fluid environments *Smart Mater. Struct.* **19** 15003
[59] Shen Q, Wang T and Kim K J 2015 A biomimetic underwater vehicle actuated by waves with ionic polymer–metal composite soft sensors *Bioinspir. Biomim.* **10** 55007
[60] Shen Q, Kim K J and Wang T 2014 Electrode of ionic polymer-metal composite sensors: modeling and experimental investigation *J. Appl. Phys.* **115** 194902
[61] Shen Q, Kim K J and Wang T 2014 Electrode of ionic polymer-metal composite sensors: modeling and experimental investigation *Proc. of SPIE—The Int. Society for Optical Engineering* p 9056
[62] Tiwari R and Kim K J 2013 IPMC as a mechanoelectric energy harvester: tailored properties *Smart Mater. Struct.* **22** 15017